Structure and functions of human oxysterol 7α-hydroxylase cDNAs and gene *CYP7B1*

Zhengliang Wu,* K. O. Martin,† N. B. Javitt,† and J. Y. L. Chiang[1,*]

Department of Biochemistry and Molecular Pathology,* Northeastern Ohio Universities College of Medicine, P. O. Box 95, Rootstown, OH 44272, and Department of Medicine,† New York University, New York, NY 10016

Abstract Oxysterol 7α-hydroxylase has broad substrate specificity for sterol metabolites and may be involved in many metabolic processes including bile acid synthesis and neurosteroid metabolism. The cloned human oxysterol 7α-hydroxylase (CYP7B1) cDNA encodes a polypeptide of 506 amino acid residues that shares 40% sequence identity to human cholesterol 7α-hydroxylase (CYP7A1), the rate-limiting enzyme in the conversion of cholesterol to bile acids in the liver. In contrast to the liver-specific expression of CYP7A1, CYP7B1 mRNA transcripts were detected in human tissues involved in steroid genesis (brain, testes, ovary, and prostate) and in bile acid synthesis (liver) and reabsorption (colon, kidney, and small intestine). The human oxysterol 7α-hydroxylase transiently expressed in 293/T cells was able to catalyze 7α-hydroxylation of 27-hydroxycholesterol and dehydroepiandrosterone (DHEA). The human *CYP7A1* and *CYP7B1* both contain six exons and five introns. However, *CYP7B1* spans at least 65 kb of the genome and is about 6-fold longer than *CYP7A1*. The transcription start site (+1) was localized 204 bp upstream of the initiation codon. No TATA box-like sequence was found near the transcription start site. Transient transfection assays of *CYP7B1* promoter/luciferase reporter constructs in HepG2 cells revealed that the promoter was highly active. The 5′ upstream region from nt −83 to +189 is the core promoter of the gene.—Wu, Z., K. O. Martin, N. B. Javitt, and J. Y. L. Chiang. **Structure and functions of human oxysterol 7α-hydroxylase cDNAs and gene *CYP7B1*. *J. Lipid Res.* 1999.** 40: **2195–2203.**

Supplementary key words bile acid synthesis • cholesterol 7α-hydroxylase • dehydroepiandrosterone (DHEA) • neurosteroids • cytochrome P450

The recent discovery of a sterol 7α-hydroxylase that differs significantly in tissue distribution and substrate specificity from cholesterol 7α-hydroxylase has introduced new concepts with respect to sterol metabolism and regulation of bile acid biosynthesis in humans (1–9). This sterol 7α-hydroxylase was initially cloned from a cDNA library of rat hippocampus (10). It was later shown to have 7α-hydroxylase activity for 27-hydroxycholesterol (11) and for dehydroepiandrosterone (DHEA) and pregnenolone in the brain (12). Thus the sterol 7α-hydroxylase with broad substrate specificity toward oxysterols is now referred as oxysterol 7α-hydroxylase.

The classic pathway of bile acid synthesis is initiated by cholesterol 7α-hydroxylase in the liver and is tightly regulated by bile acid feedback, hormones, and diurnal rhythm (2). In contrast, the pathway initiated with sterol 27-hydroxylase is located mainly in extrahepatic tissues, such as kidney, macrophage, and vascular endothelium. The 27-hydroxycholesterol is then 7α-hydroxylated by oxysterol 7α-hydroxylase and is finally converted to chenodeoxycholic and cholic acid in the liver. The absence of 7α-hydroxylation would lead to formation of monohydroxy bile acids. Although in adults this alternative (or acidic) pathway makes a quantitatively minor contribution to total bile acid synthesis, it may represent a significant mechanism for preventing the development of atherosclerosis (13).

Oxysterol 7α-hydroxylase activity expressed after 18 days of life might be responsible for the synthesis of 7α-hydroxylated bile acids in *cyp7a* (−/−) mice (14). The accumulation of a high level of monohydroxy bile acids in newborn *cyp7a* (−/−) mice (5 to 10 days), the result of absence of both cholesterol 7α-hydroxylase and oxysterol 7α-hydroxylase activities, might cause severe neonatal cholestasis (15). We previously identified a metabolic defect in the 7α-hydroxylation of 3β-hydroxy-Δ^5-cholestenoic acid in a child with neonatal cholestasis (16). This has led us to isolate cDNA and the gene encoding human oxysterol 7α-hydroxylase. Our study revealed the structure of the human *CYP7B1* and its functions in the metabolism of neurosteroids and oxysterols and provided important molecular tools for studying the mechanism of oxysterol metabolism and the cause of cholestatic liver disease in humans.

Abbreviations: *CYP7B1*, oxysterol 7α-hydroxylase gene; *CYP7A1*, cholesterol 7α-hydroxylase gene; DHEA, dehydroepiandrosterone; DMEM, Dubecco's modified Eagle's medium; Luc, luciferase; CMV, cytomegalovirus; PCR, polymerase chain reaction; RLU, random light units; kb, kilobases; nt, nucleotide.

[1] To whom correspondence should be addressed.

EXPERIMENTAL PROCEDURES

cDNA library screening

Plasmid pcDNA3.1 (+)-mcyp7b (11) containing a mouse cyp7b1 cDNA was digested with *Hind*III and *Bgl*II to release a 477 bp fragment from the 5′ region of the coding sequence. A random primer labeling kit (RadPrimer DNA Labeling System, Life Technology, Gaithersburg, MD) was used to label the probe with [α-^{32}P]dCTP. A human hippocampus λgt10 cDNA library (Clontech, Palo Alto, CA) and a human liver λZAP cDNA library (Stratagene, La Jolla, CA) were plated. About 10^6 plaque-forming units of each library were screened in each study. Positive clones were plaque-purified and phage DNAs were isolated using a Nucleobond Lambda kit (Clontech). The cDNA inserts were released with *Eco*RI and were subcloned into pBlueScript KS (II+) vector. The purified λZAP clones were excised in vivo from phage DNA and circularized to form a phagemid by co-infection of a f1 helper phage with host *E. coli* strain XL1-Blue.

Cloning the human *CYP7B1*

A human placenta genomic λFIX II library (Stratagene) was screened for CYP7B1 genomic clones. The cloned phage DNAs were cut with *Xba*I and run on a 1% agarose gel. The size of each clone was estimated by adding up all *Xba*I fragments. A restriction map of the gene was determined by analysis of number *Xba*I fragments of each individual clone by Southern blot hybridization using cDNA probes. *Xba*I fragments containing exons were then subcloned into pBlueScript KS (II+) vector, cut with *Xba*I, and sequenced. The sizes of the introns were estimated by adding up all *Xba*I fragments between two exons and were later confirmed by genomic PCR. Several rounds of screening obtained clones that contained intron 1. The 5′-*Xba*I fragment of a genomic clone (G17) containing exon 2 and closest to the 5′ end was identified and was then used as a probe to again screen the genomic library for upstream clones. Those clones were analyzed by restriction analysis to identify the *Xba*I fragment closest to the 5′ end. This screening was repeated to obtain a genomic clone (G30), the 5′ end of which overlaps the 3′ end of the genomic clone (G43) that contains exon 1 and the 5′-flanking sequences.

Determining the *CYP7B1* structure

An Advantage Genomic PCR kit (Clontech) was used for polymerase chain reactions (PCR) to locate exons and to determine the sizes of introns. Genomic clones that contained two adjacent exons were used as templates for PCR. Pairs of primers approximately 30 nucleotides each were designed according to the donor and acceptor exon sequences. The intron sequence was amplified and PCR products were analyzed on agarose gels. Intron/exon junction sequences were determined by DNA sequencing. Intron 1 was too big to be determined by PCR. The size of intron 1 was then estimated by restriction analysis of overlapping intron 1 clones obtained as described above.

DNA preparation and sequencing

All plasmids and phage DNA samples were prepared with Nucleobond AX columns (Clontech). A Sequenase Version 2.0 DNA sequencing kit (USB, Cleveland, OH) was used for nucleotide sequencing. Sequencing primers were designed from previously determined sequences and were used for further sequencing of both strands of DNA. Sequences in the GC-rich region were determined using both dITP and dGTP.

Northern blot hybridization analysis

Two human multiple tissue mRNA blots MTN-I (#7760-1) and II (#7759-1)(Clontech) were used to detect CYP7B1 mRNA transcripts in human tissues. The full-length human CYP7B1 cDNA was used as a probe and hybridization was carried out according to manufacturer's instructions. Radioactivity was detected by scanning with a phosphorimager (Model 455si, Molecular Dynamic, Sunnyvale, CA). Radioactivity was then washed out and the membrane was rehybridized with a CYP7A1 cDNA probe. β-Actin was probed as an internal standard for normalization of RNA levels in each tissue.

Expression vector construction

A full-length human CYP7B1 cDNA was isolated from a phage clone λH107 and was subcloned into pBluescript KS (II+). The recombinant plasmid pH107 was digested with *Sma*I and *Eco*RV to release a 1.6 kb fragment, which contains all but the codons for the first 20 amino acids. This fragment was then cloned into pcDNA3.1/His A plasmid (Invitrogene, Portland, OR) cut with *Eco*RV. Restriction analysis and DNA sequencing determined the orientation of the insert in the plasmid. The clone containing the insert in the forward direction was named pΔ20hCYP7B1 and that with the sequence in the reverse direction was called pΔ20hCYP7B1R. The DNA fragment containing the full-length coding sequence was released from pH107 with *Kpn*I and *Xba*I and was subsequently subcloned into pcDNA3 (Invitrogene, Portland, OR) cut with *Kpn*I and *Xba*I. The recombinant plasmid was named phCYP7B1.

Determination of transcription start site

Oligonucleotide primer (5′-CTAGTCCAGGGCCGGAGAGGC TGGCCTGC-3′) corresponding to the complimentary sequence of nt 105 to 77 was used for primer extension. Primers were labeled with [γ-^{33}P]dATP (NEN Life Science, Beverly, MA). Assays were done using a Primer Extension kit from Promega (Madison, WI). Ten pmol of radiolabeled primer was annealed to 1 μg of human hippocampus poly A (+) RNA (Clontech) at 60°C for 1 h in primer extension buffer (50 mM Tris, pH 8.3, 50 mM KCl, 10 mM $MgCl_2$, 10 mM DTT, 1 mM each of dNTP, 0.5 mM spermidine). Reverse transcription was carried out by avian myeloblastosis virus (AMV) reverse transcriptase (Promega) for 30 min at 42°C. Loading dye was added into each reaction and the reverse transcription products were analyzed on 8% polyacrylamide gel electrophoresis in 8 M urea, along with sequencing reactions using the same primer. The gel was run until bromophenol blue was close to the bottom of the gel. The gel was dried and radioactivity was scanned with phosphorimager.

Computer analysis

All the sequence alignment, restriction enzyme mapping, PCR primer design, and amino acid translation studies were done with MacVector software (Oxford Molecular Biology, Oxford, England). Binding sites for putative transcription factor were identified using the TRANSFAC program (http://transfac.gbf.de/Transfac/MatInspector).

Expression of hCYP7B1 and enzyme activity assay

Human kidney 293/T cells derived from ATCC293 were grown and maintained in DMEM with 10% fetal bovine serum. 293/T cells were plated in 6-well plates 1 day before the transfection (11). For transfection, freshly prepared calcium phosphate precipitate (1.25 μg plasmid/well) was added to 293/T cells that were 60–70% confluent and was allowed to remain in contact with the cells for 24 h. The media containing the DNA were removed. The cells were washed with phosphate-buffered saline, 2 ml of fresh media containing 15% D_2O and 10% delipidated fetal calf serum, and 5 mM 27-hydroxycholesterol, cholesterol, or 13.4 μM DHEA were added, and the mixture was incubated for an additional 24 h. The media were then used for HPLC analysis. The amounts of the substrate and product were calculated from

the peak area in HPLC spectra. Activity was calculated in terms of nmole product per mg protein per 24 h.

Construction of promoter/luciferase reporter genes and transient transfection assay

The upstream sequence from *Hind*III (nt − 1082) to *Sac*II (+189) was released from pBluescript KS (II+) with *Kpn*I and *Sac*I and was subcloned into pGL3 Basic luciferase reporter plasmid (Promega). The 5′ deletion mutants (p-343/+189-Luc, p-291/+189-Luc, and p-144/+189-Luc) were generated with the pBluescript II Exo/Mung DNA Sequencing System (Stratagene). Three constructs (p1082/-84Luc, p-857/-84Luc, and p-291/-84-Luc) were also made by deletion of a *Sma*I fragment from the 3′ end of the constructs. Transient transfection assays were performed as described previously with some modification (17). HepG2 cells were cultured in DMEM supplemented with 10% fetal bovine serum in 12-well plates. At 70% confluence, the cells were transfected with 2.5 μg DNA together with 150 ng of pCMVβ, an expression plasmid for β-galactosidase, as an internal control for transfection efficiency. After incubation for 2 days, the cells were harvested and lysed with lysate buffer. A 20-μl aliquot of lysate was used to assay luciferase activity with Luciferase Assay System (Promega). Ten μl of each lysate was also assayed for β-galactosidase activity by incubating with *o*-nitrophenyl-β-d-galactopyranoside at 37°C for 30 min and measuring absorbance at 405 nm. Luciferase reporter activity was expressed as random light units (RLU) divided by β-galactosidase activity.

RESULTS

Cloning human CYP7B1 cDNAs

To clone human CYP7B1 cDNA, a 5′-fragment of mouse cyp7b1 cDNA was used as a hybridization probe to screen a λgt 10 cDNA library of human hippocampus. Three full-length cDNA clones H20 (5kb), H25 (1.7 kb), H107 (2.1 kb) were obtained and restriction maps were determined, as well as the nucleotide sequence of clone H107 (GenBank Accession #AF127090). H107 contains an open reading frame of 1521 bp, which encodes a peptide of 506 amino acids. The longest clone (H20) obtained is 5 kb in length and contains more than 3 kb of the 3′ untranslated region (UTR). Sequence analysis revealed that human CYP7B1 shared 64.6% amino acid sequence identity with mouse cyp7b1 (10) and 40.4% identity with human CYP7A1 (18). The N-terminal membrane-binding domain (amino acid residues 1 to 38) is highly hydrophobic. The nucleotide coding sequences show 72.6% and 49.2% identity with the mouse cyp7b1 and human CYP7A1, respectively. The clones obtained from a cDNA library of human hippocampus all lack a poly A (+) tail because the library was constructed by a random priming method. Ten partial-length CYP7B1 clones were also isolated from a cDNA library of human liver constructed by oligo dT-priming. These clones lacked 5′-coding sequences and all contained a poly (A+) tail. The nucleotide sequences of these liver cDNA clones were identical to the corresponding sequences of the hippocampus cDNA clones.

Setchell et al. (19) reported cloning a human CYP7B1 cDNA. Comparison with the cDNA and amino acid sequences found by these investigators and those found in our studies revealed one base-pair difference at codon 324, which codes for His (CAT) and Arg (CGT), respectively.

The GC content of the 281-bp nucleotide sequences of the 5′-region of human cDNA is 74.4%. This is well above the average GC content of 56% for human genes around the initiation codon (20). Two putative polyadenylation signals were noticed in 3′UTR. One (AATAAA) was located 19 bp and the other (AATAAA) 284 bp downstream of the stop codon. Indeed, nucleotide sequences of the cDNA clones obtained revealed that both polyadenylation signals were utilized in poly A (+) mRNA synthesis. However, all liver clones lacked the GC-rich 5′ sequence. This could be because the secondary structures of the 5′ GC-rich region prevented the continuation of synthesis of the full-length first-strand cDNA from mRNA templates by reverse transcriptase when oligo dT was used for priming.

Cloning the human *CYP7B1*

As the *CYP7A1* we had previously cloned were approximately 10 kb, we had expected that the *CYP7B1* would be similar in size. The same human placenta λFIXII genomic library was screened using a full-length human CYP7B1 cDNA. A total of 18 positive clones were obtained by screening approximately 2 million plaque-forming units. Six overlapping genomic clones used to construct the gene structure are shown in **Fig. 1**. The *Xba*I fragments containing exons were identified using cDNA fragments as hybridization probes. The exon/intron junction sequences in these fragments were then determined using primer pairs designed according to the exon sequences. The exon/intron junction sequences and the sizes of each exon and intron are presented in **Table 1**. All donor and acceptor sites of exon/intron junction sequences follow the GT/AG rule. The sizes of introns were determined as described above in Material and Methods. The size of intron 1 was estimated to be approximately 30 kb by adding up all *Xba*I fragments between exon 1 and exon 2. The minimum size of *CYP7B1* was estimated to be 65 kb.

Multiple tissue Northern blot analysis

Human multiple tissue Northern blots were hybridized with the full-length human CYP7B1 cDNA probe. A single band approximately 9 kb long was seen in all tissues (**Fig. 2A**, MTN-I). The levels of CYP7B1 mRNA expression were estimated after normalizing with β-actin signal and were in the order of liver > brain = kidney = pancreas > heart > lung > skeletal muscle > placenta. In another tissue blot (Fig. 2B, MTN-II), 9 kb mRNA transcripts were detected in ovary, testes, prostate, colon, small intestine, and thymus. mRNA species of approximately 2.5 kb in length were also detected in human liver and testes. The human CYP7B1 mRNA transcripts are much longer than those found in mouse and rat, which were reported to be about 2kb (10, 21). The same blot was stripped of radioactivity and was then re-probed with human CYP7A1 cDNA. A band of approximately 4 kb was found only in liver.

Cloning the 5′ flanking upstream region of the human *CYP7B1* and mapping the transcription start site

The genomic clone G43 contained 19 kb of the gene. A 10 kb *Xba*I fragment containing exon 1 was isolated and

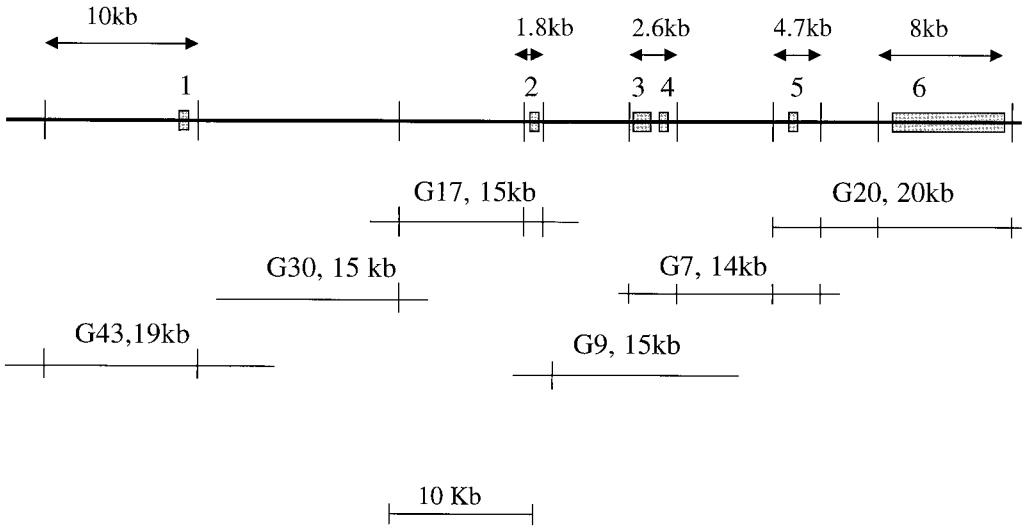

Fig. 1. Gene structure of human *CYP7B1*. The *CYP7B1* contains 6 exons (boxes) and 5 introns (lines between two exons), and spans about 65 kb. The intron sizes are drawn to scale, but the exons are not. Six genomic clones, which were used to determine gene structure, are shown below the gene. *Xba*I (X) restriction fragments used to determine the exon/intron junction structure are indicated.

further mapped (**Fig. 3A**). Nucleotide sequences from *Hind*III to the initiation codon ATG are shown in Fig. 3B. Using human hippocampus mRNA as a template, the transcription start site was mapped to a G located 204 bp upstream of the initiation codon (**Fig. 4**). A perfect GC box sequence is located just upstream of the transcription start site.

The clone G43 contained approximately 9 kb of the 5′upstream sequence. Analysis of the 1.3 kb sequence with the MatInspector program (http://transfac.gbf.de/cgi-bin/matSearch/matsearch.pl) (22) revealed several putative transcription factor-binding sites. No canonical TATA box sequence was found in the region approximately 50 bp upstream of the transcription start site (+1), but CAAT and GC box sequences were found at nt −105 and −26, respectively. A typical TATAAAA sequence was found between nt −709 and −703, which was far upstream of the transcription start site we had determined. Two overlapping sterol response element (SRE)-like sequences (CACCCCAC) were found to be located between nt −327 and −314 (23). Other putative transcription factor binding sequences such as NFAT (24), C/EBPβ, NFκB (25), GATA box (26), HNF3β (27), NF1 (28), and AP4 were identified.

Alignment of the corresponding 5′-upstream regions of the human *CYP7B1* and *CYP7A1* showed a very low sequence identity, less than 30%. The *CYP7B1* promoter was found to have a GC content of 65% in the region of 500 bp upstream of the transcription start site, whereas that of the *CYP7A1* was only 45%.

Transient transfection assays of *CYP7B1*/luciferase constructs

To identify the promoter and map the *cis*-regulatory elements in the 5′-flanking region, eight deletion constructs of *CYP7B1* promoter/luciferase reporter genes were tran-

TABLE 1. Human *CYP7B1* structure

Exons	5′ Ends of the Introns	Introns	3′ Ends of the Introns	Codons at the Junction Sites
1 (>280 bp a.a. 1–41)	TTGTCCGGCGCACCAGgtaag		tttttatctttttttttttccttgtagGAGAC	R411
	cgcctcggccgccacgacgcatgcgc	~30 kb	CCGGTGAGCCTCCATT	AGG
2 (137 bp a.a. 41–87)	CTTTCACAGTTCTTCTTGGT		ttttttttttctagGAAAGTACATA	G87
	Ggtaagaagcacttctataataccttatata	8 kb	ACATTTATCCTGGA	GGA
3 (591 bp a.a. 87–284)	TGCACGAGGACCTTGAAAT		ttaatcttccttttcacttattttctcccagC	A284
	AGGAGgtaagaacttctgaatgagcac	0.5 kb	ACATCATTTAGGCTTTCT	GCA
4 (207 bp a.a. 284–353)	TTGGACAGCCTAATCTGCC		ttaataagctatcgtttgtttttttccttcagA	E353
	TAGgtaatttatttttatctgttatgaagaaaa	11 kb	AAGCAGCATTTTTGAA	GAA
5 (176 bp a.a. 353–411)	TTTGAAGCTCTCCAGAGgtaag		aaatgttaattttaacactattccttccttac	E411
	taaacatcaagcctat	8 kb	agGAGTTTAGATATGATC	GAG
6 (>793 bp a.a. 412–506)				

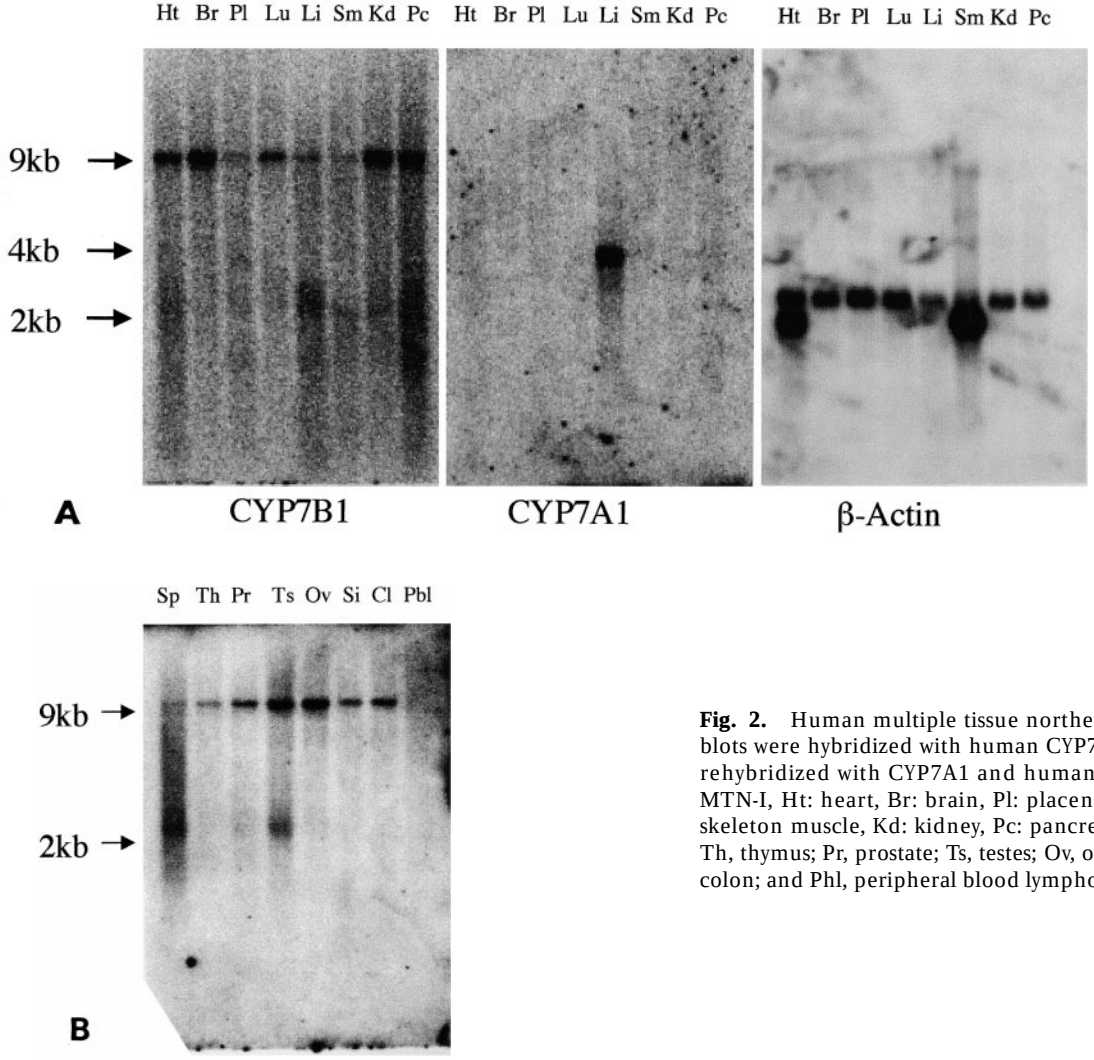

Fig. 2. Human multiple tissue northern blot hybridization. The blots were hybridized with human CYP7B1 cDNA probe and then rehybridized with CYP7A1 and human β-actin cDNA probes. A: MTN-I, Ht: heart, Br: brain, Pl: placenta, Lu: lung, Li: liver, Sm: skeleton muscle, Kd: kidney, Pc: pancreas. B: MTN-II, Sp, spleen; Th, thymus; Pr, prostate; Ts, testes; Ov, ovary; Si, small intestine; Cl, colon; and Phl, peripheral blood lymphocyte.

siently transfected into HepG2 cells. **Figure 5** shows that the *CYP7B1* promoter was very active, comparable with the SV40 promoter. Deletion of the 5′-flanking sequence from −1082 to −291 did not affect reporter activity. Deletion of the sequences between −291 and −87 decreased activity by about 45%, indicating that the deleted region may contain binding sites for the *trans*-activator. Deletion of the sequence from −83 to +189 resulted in complete loss of transcriptional activity for these reporter constructs, indicating that the sequences from −84 to +189 are essential for promoter activity. A perfect GC box is located in this region (Fig. 3). The GC box binds SP-1, a ubiquitous transcription activator involved in transcriptional regulation of many genes. These results suggest that a TATA box sequence located at −719 is not likely to play a functional role in initiation of transcription by RNA polymerase II. Nucleotide sequences from −291 to −87 contain positive *cis*-regulatory elements. Putative binding sites for C/EBPβ, CAAT box, NF-κB are located in this region. These sequences are likely important for transcriptional activity of the *CYP7B1* promoter. Experiments are in progress to further identify *cis*-regulatory elements in the 5′-flanking region of the gene in different tissues.

Transfection assays of enzyme activities expressed by CYP7B1 cDNA

To provide evidence that the human CYP7B1 cDNA we cloned does express oxysterol 7α-hydroxylase activity, expression plasmids carrying a full-length (phCYP7B1) and a truncated (pΔ20hCYP7B1) CYP7B1 cDNA were transiently transfected into 293/T cells and enzyme activities toward 27-hydroxycholesterol and DHEA were measured in lysates of the transfected cells. With 27-hydroxycholesterol as a substrate, the full-length and truncated enzymes expressed in 293/T cells produced 0.6 and 0.8 nmol 7α, 27-dihydroxycholesterol per mg protein per 24 h, respectively (**Table 2**). In contrast, with DHEA as a substrate, the full-length and truncated enzymes produced 85 and 89 nmol 7α-hydroxyDHEA/mg protein/24 h, respectively, activities that were approximately 100-fold greater than those with 27-hydroxycholesterol. The plasmid carrying a cDNA cloned in the reverse direction (pΔhCYP7B1R) did not express any enzyme activity at all. Activities of the truncated and full-length enzymes were similar toward both the above substrates, indicating that the N-terminal membrane-binding domain may not be re-

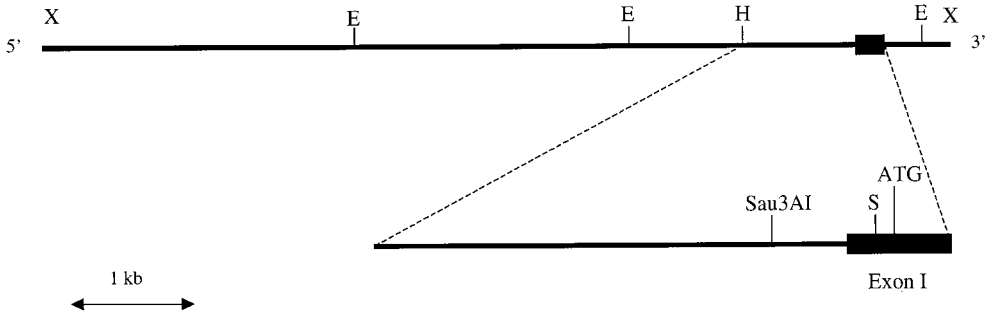

Hind III

-1085 AAGCTTGAGTATATATATG GAACC GTTCTGGCGAGGGGAGTTGTA CAATGAAGACAATTT
-1025 GTGCAGGGCTTCTCATTGC AGGTGGAGGATATGACTTCGTCACAAA GA CAACCATTAAGA
-965 GTTTTGAACAGAGTAAAAGCTGGAGAGGTCTGTGTTTTAGGGA GGTGGAAATGGGGATGA
-905 TGGACTGGAAGGGTAAAAAACCAGAGATTGGTTTTGAAGCTGC TGTACC CATTCCAGAGA
-845 AGTGTTGCATTGACAGAGCACACAAGTCCTCGAATAGGACCGTGG TTAGAAC GGCCGATA
GATA1
-785 TTTATCAGTGGG AATGGTAAACAT TTATCAAGTGAG CAAC CAAGT TCAGTTACTTAATCT
-725 GAG TCTCATTATGTCTTCTATAAAATACACATTAAAAATAGAAAG TAAAAACGTG GGTAA
TATA like
-665 AGTAC CCA GTGGATG GTCATTACTCAGAAAAAGGTATTTTAAAA GTTTC TCC CTTATTCT
-605 TTC TGAGTA CAACCTG TAGTACTTGAACCAC TTCTCTTTC GTCC CCTA CCAC GCTGTTCT
-545 GCAATCTCTTTTTAC CTGT CTCA C TCTCTTCCT GTAC TGT GTGCC TCATCG GGACTTCTA
-485 AAGGCTTACG GCCTAG GTCTTT GTATTCC GTGTCTCTGGCACGCGCCT CTG CACACAGCA
NF1
-425 GGCCTGAACCAAAACTTGTGAGCAAATAGGATGCAAGGGGGTGAAGGAGGTGGGCGCGAA
HNF-3B
-365 ACGGGTTCGAGGTCGC GCACTCC GCCGGTTTCTGC CGCCAGCCCAACCCGCTG GGTCGTA
SRE
-305 CCTAAGAGATCGCCGGTG TCAGAGCGCAGCGGGCACCTTCACAAGCATC TTGAG GGACAA
AP4
-245 GCAGAGTCGCTCCTCGCAGGGCGCGGGCTAAGAAGTGAGGAACCCAAGGGGCT CCCGTCC
-185 AACTAAGAAGCGAAATCCCCC ACCTCCAG GCCTTCAGGGCT GGTTCTTGGGAAATCCTAA
NF-κB
CEBPB
-125 CTCTTTCCCTTC TAACCCC TTCCTTGGCCCTTC TTCC TGCCC GGGA GGATCAAGGGCGCT
CAAT BOX
-65 GTTTTCCAGAAGCTGCCGGGTCGGAAACGGTGGGGGGAACGGGGCGGTACGCGTGGGTGGA
NFAT
GC BOX
*
-5 GGATAGGCGGGGAGGGGGCAGTCCACGAACTTTTGTCATTCAGCCTGGGAGACCACGGTG
56 ACATTCCTGTCTGCGCTGCGGGCAGGCCAGCC TCTCCGGCCCTGGACTA GGGGGCGCCGC
116 CGAGAGAAGCCGCCGCAGGCTGCAGAGTCGCCGACCGCGCTGTTCGCAGGCAGACCCCGG
176 GCTGCCCACCGCGGCCTAGCGCGCGCCGGATG

Fig. 3. The nucleotide sequences of the 5′-upstream region of the human *CYP7B1*. Top: Restriction map of a 10 kb *Xba*I fragment which contains exon 1 and 9 kb upstream sequence was obtained from genomic clone G43. The 1.3 kb *Hind*III, *Sac*II fragment was further subcloned and sequenced. X: *Xba*I, E: *Eco*RI, H: *Hind*III, S: *Sac*II. Bottom: The 5′-upstream sequences of human CYP7B1 gene. The transcription start site (+) G is located 204 nucleotides upstream of ATG start codon. A reversed CAAT box and a GC box are located. Putative binding sites for transcription factors were identified by computer analysis and are underlined and labeled. Sterol response element (SRE)-like sequences are also identified. GenBank accession #127089.

quired for catalytic activity, similar to the finding for cholesterol 7α-hydroxylase (29). These data provided further evidence that the human CYP7B1 clone we isolated does encode oxysterol 7α-hydroxylase.

DISCUSSION

It is rather surprising from our study that the CYP7B1 mRNA and its gene are much larger than *C*YP7A1 al-

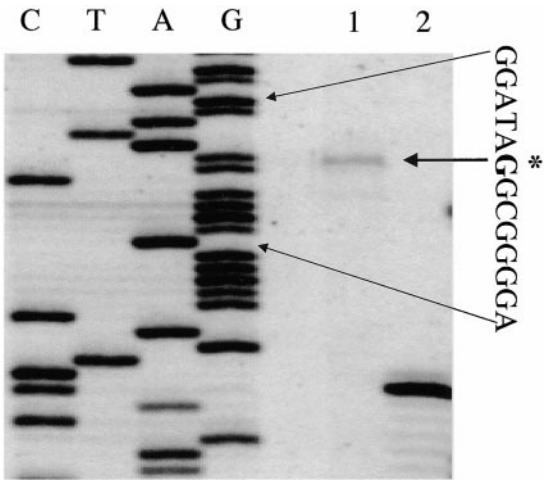

Fig. 4. Primer extension assay of the transcription start site. Human hippocampus poly A (+) RNA was used as a template for primer extension assay as described under Experimental Procedures. Sequencing reactions with the same primer used for primer extension assay were run on the same gel and are shown. Lane 1, primer extension reaction with 1 μg of human hippocampus poly A (+) RNA. Lane 2, a positive control reaction with a 1.2 kb Kanamycin mRNA and primer provided in primer extension kit.

though the intron/exon structures of the two are very similar. These two genes are in close proximity on human chromosome 8 (19). It is likely that the more compact *CYP7A1* may be derived from the *CYP7B1* by an ancient gene duplication or gene conversion event, and cholesterol 7α-hydroxylase was selectively expressed only in the liver for bile acid synthesis. On the other hand, oxysterol 7α-hydroxylase mRNA transcripts are expressed in tissues involved in steroidogenesis and neurosteroid metabolism (testes, ovary, prostate, kidney, liver, and brain) and in tissues involved in bile acid synthesis (liver) and absorption (small intestine, kidney, and colon). This may imply that oxysterol 7α-hydroxylase may have multiple functions, including bile acid synthesis, neurosteroid metabolism, sex hormone synthesis, and detoxification of oxysterols.

The size of oxysterol 7α-hydroxylase mRNAs in all tissues is approximately 9 kb, which is much longer than cholesterol 7α-hydroxylase. The coding sequences of both hydroxylases are about the same. As the transcription start site is located 204 bp upstream of the initiation codon, the exon 6 of oxysterol 7α-hydroxylase could be as long as 7 kb. The longest cDNA we isolated was 5 kb. It would be extremely difficult to isolate a full-length cDNA clone of 9 kb long. The human CYP7B1 shows a 64.6% amino acid sequence identity with the mouse cyp7b1. This is typical for cytochrome P450 genes in the same subfamily (30). The similarity in enzyme activity and substrate specificity between human and mouse enzyme supports the concept that the human CYP7B1 we cloned is the mouse homologue. The presence of multiple oxysterol 7α-hydroxylase activities has been suggested (31). However, all human CYP7B1 clones we isolated from cDNA libraries of the liver and hippocampus using mouse cyp7b1 and human CYP7B1 cDNA as probes are identical in nucleotide sequences. The human CYP7B1 cDNAs we cloned and that

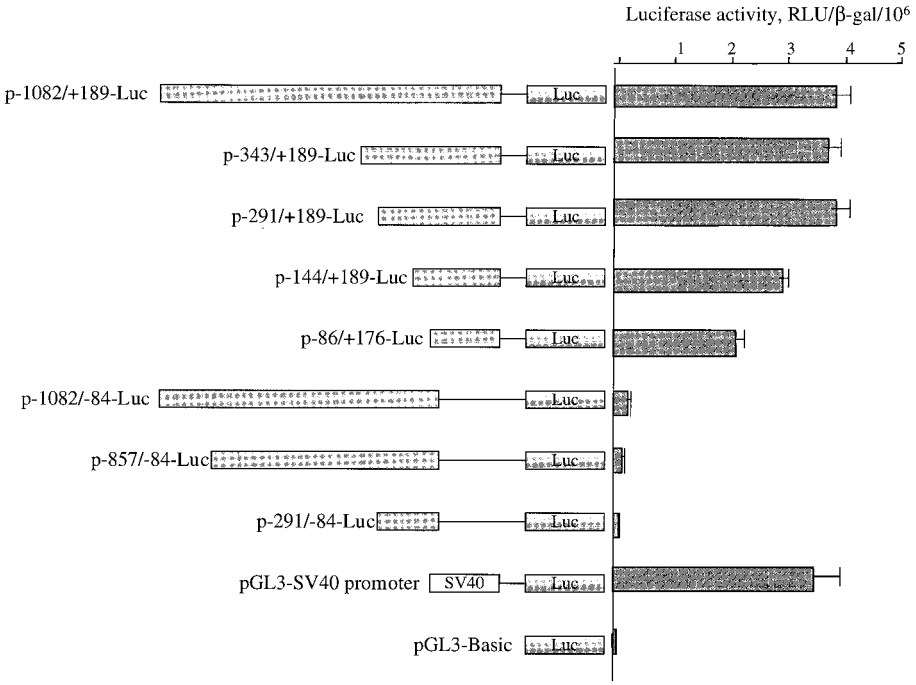

Fig. 5. Transient transfection assays of *CYP7B1* promoter/luciferase reporter gene constructs in HepG2 cells. *CYP7B1* promoter/luciferase reporter gene constructs were cotransfected with pCMVβ into HepG2 cells. The luciferase activity and β-galactosidase activity were measured 2 days later. Luciferase activity is expressed as random light unit (RLU) divided by β-galactosidase activity. Error bar represents standard deviation of triplicate samples.

TABLE 2. Expression of oxysterol 7α-hydroxylase activity in 293/T cells

Plasmid Constructs	Activity: 27-Hydroxycholesterol (7α, 27-dihydroxycholesterol)	Activity: Dehydroepiandrosterone (DHEA) (7α-hydroxyl DHEA)
	nmol/mg of protein/24 h	
pΔ20hCYP7B1R	0	0
pΔ20hCYP7B1	0.82 ± 0.12	89.1 ± 13.6
phCYP7B1	0.62 ± 0.01	84.5 ± 44.0

were isolated by PCR are identical except for one nucleotide difference (19). It is unlikely that the human oxysterol 7α-hydroxylase we isolated is a third isoform of the CYP7 family. This does not rule out the presence of a third form of oxysterol 7α-hydroxylase, however.

Setchell et al. (19) recently reported an inborn error of bile acid metabolism caused by a point mutation in the Arg 388 codon of oxysterol 7α-hydroxylase that resulted in premature termination. This neonate had severe cholestasis and cirrhosis. The defect in 7α-hydroxylation was revealed by the absence of primary bile acid conjugates and the presence of high levels of 3β-hydroxy-Δ^5-cholenoic and cholestenoic acids in the serum and urine, the metabolites formed via the acidic pathway of bile acid biosynthesis. Cholesterol 7α-hydroxylase activity was also absent in this patient. The probable cause of the liver injury was the accumulation of high levels of hepatotoxic monohydroxy bile acids, 24, 25, and 27-hydroxycholesterols. Thus a physiological function of oxysterol 7α-hydroxylase is to protect liver from cholestasis in neonatal life (16, 19).

Oxysterols are found in human serum, macrophages, vascular endothelium, and atherosclerotic plaques (32) and are potent inhibitors of expression of the genes encoding low density lipoprotein receptor, 3-hydroxy-3-methylglutaryl-CoA reductase, and other enzymes in the mevalonate pathway (33). Recently, oxysterols were identified as ligands for the liver orphan receptor (LXR), which has been suggested to function in a signaling pathway for regulating cholesterol and bile acid biosynthesis (34). Thus, sterol hydroxylases in bile acid biosynthesis pathways play important roles in cholesterol homeostasis. As oxysterol 7α-hydroxylase has broad substrate specificity, it may metabolize cytotoxic oxysterols to dihydroxy metabolites, which are more soluble and readily excreted from extrahepatic tissues, diffused into circulation, transported into liver, and converted to bile acids, presumably by acidic bile acid biosynthesis pathway.

DHEA and pregnenolone are active neurosteroids that play roles in neuronal development and activation of N-methyl-d-aspartate receptor (35, 36). The 7α-hydroxylation of DHEA is a quantitatively important metabolic step in brain tissue and may contribute to the regulation of the concentration and activity of neurosteroids in brain (37).

Although the recognition of a novel 7α-hydroxylase enzyme resulted from studies of pathways of bile acid synthesis, it is unlikely that oxysterol 7α-hydroxylase functions as a key regulatory enzyme like cholesterol 7α-hydroxylase. In contrast to cholesterol 7α-hydroxylase, oxysterol 7α-hydroxylase does not initiate bile acid synthesis and its activity is much higher than that of cholesterol 7α-hydroxylase in human liver (4). It is not known whether oxysterol 7α-hydroxylase activity is regulated by bile acids, oxysterols, or other factors. Results from transient transfection assay of the *CYP7B1*/luciferase reporters in HepG2 cells have defined the nucleotide sequences essential for the transcriptional activity of the promoter to a 272 bp fragment in the 5′-upstream region. Recently, FXR has been identified as a bile acid receptor, which mediates the negative feedback regulation of CYP7A1 gene transcription (38–40). Preliminary study from this laboratory showed that FXR and bile acids do not regulate the *CYP7B1* transcription. This study provides us with important molecular tools for studying the mechanism of regulation of the acidic bile acid biosynthesis pathway in the liver, the pathogenesis of cholestatic liver diseases, and the regulation of steroid metabolisms in brain and other tissues.

This research was supported by grants GM31584 and DK44442 from the National Institutes of Health. The technical assistance and discussion of Dr. Diane Stroup and editorial assistance of Mrs. Suzanne Javitt are gratefully acknowledged.

Manuscript received 13 May 1999 and in revised form 24 August 1999.

REFERENCES

1. Javitt, N. B. 1994. Bile acid synthesis from cholesterol: regulatory and auxiliary pathways. *FASEB J.* **8:** 1308–1311.
2. Chiang, J. Y. L. 1998. Regulation of bile acid synthesis. *Front. Biosci.* **3:** D176–193.
3. Shoda, J., A. Toll, M. Axelson, F. Pieper, K. Wikvall, and J. Sjovall. 1993. Formation of 7α- and 7β-hydroxylated bile acid precursors from 27-hydroxycholesterol in human liver microsomes and mitochondria. *Hepatology.* **17:** 395–403.
4. Bjorkhem, I., B. Nyberg, and K. Einarsson. 1992. 7α-hydroxylation of 27-hydroxycholesterol in human liver microsomes. *Biochim. Biophys. Acta.* **1128:** 73–76.
5. Axelson, M., J. Shoda, J. Sjovall, A. Toll, and K. Wikvall. 1992. Cholesterol is converted to 7α-hydroxy-3-oxo-4-cholestenoic acid in liver mitochondria. Evidence for a mitochondrial sterol 7α-hydroxylase. *J. Biol. Chem.* **267:** 1701–1704.
6. Martin, K. O., K. Budai, and N. B. Javitt. 1993. Cholesterol and 27-hydroxycholesterol 7α-hydroxylation: evidence for two different enzymes. *J. Lipid Res.* **34:** 581–588.
7. Toll, A., J. Shoda, M. Axelson, J. Sjovall, and K. Wikvall. 1992.7α-Hydroxylation of 26-hydroxycholesterol, 3β-hydroxy-5-cholestenoic acid and 3β-hydroxy-5-cholenoic acid by cytochrome P-450 in pig liver microsomes. *FEBS Lett.* **296:** 73–76.
8. Zhang, J., O. Larsson, and J. Sjovall. 1995. 7α-Hydroxylation of 25-

hydroxycholesterol and 27-hydroxycholesterol in human fibroblasts. *Biochim. Biophys. Acta.* **1256:** 353–359.
9. Zhang, J., Y. Akwa, E. E. Baulieu, and J. Sjovall. 1995. 7α-Hydroxylation of 27-hydroxycholesterol in rat brain microsomes. *C. R. Acad. Sci. Ser. III, Sci. Vie.* **318:** 345–349.
10. Stapleton, G., M. Steel, M. Richardson, J. O. Mason, K. A. Rose, R. G. M. Morris, and R. Lathe. 1995. A novel cytochrome P450 expressed primarily in brain. *J. Biol. Chem.* **270:** 29739–29745.
11. Martin, K. O., A. B. Reiss, R. Lathe, and N. B. Javitt. 1997. 7α-Hydroxylation of 27-hydroxycholesterol: biologic role in the regulation of cholesterol synthesis. *J. Lipid Res.* **38:** 1053–1058.
12. Rose, K. A., G. Stapleton, K. Dott, M. P. Kieny, R. Best, M. Schwarz, D. W. Russell, I. Bjorkhem, J. Seckl, and R. Lathe. 1997. Cyp7b, a novel brain cytochrome P450, catalyzes the synthesis of neurosteroids 7α-hydroxy dehydroepiandrosterone and 7α-hydroxypregnenolone. *Proc. Natl. Acad. Sci. USA.* **94:** 4925–4930.
13. Bjorkhem, I., O. Andersson, U. Diczfalusy, B. Sevastik, R-j. Xiu, C. Duan, and E. Lund. 1994. Atherosclerosis and sterol 27-hydroxylase: evidence for a role of this enzyme in elimination of cholesterol from human macrophages. *Proc. Natl. Acad. Sci. USA.* **91:** 8592–8596.
14. Schwarz, M., E. G. Lund, K. D. R. Setchell, H. J. Kayden, J. E. Zerwekh, I. Bjorkhem, J. Hertz, and D. W. Russell. 1996. Disruption of cholesterol 7α-hydroxylase gene in mice: II. Bile acid deficiency is overcome by induction of oxysterol 7α-hydroxylase. *J. Biol. Chem.* **271:** 18024–18031.
15. Arnon, R., T. Yoshimura, A. Reiss, K. Budai, J. H. Lefkowitch, and N. B. Javitt. 1998. Cholesterol 7α-hydroxylase knockout mouse: a model for monohydroxy bile acid-related neonatal cholestasis. *Gastroenterology.* **115:** 1223–1228.
16. Javitt, N. B., A. Kok, and M. Gut. 1984. Neonatal cholestasis: identification of a metabolic error in bile acid synthesis. *Pediatr. Res.* **18:** Abstract #627.
17. Crestani, M., D. Stroup, and J. Y. L. Chiang. 1995. Hormonal regulation of the cholesterol 7α-hydroxylase gene (CYP7). *J. Lipid Res.* **36:** 2419–2432.
18. Karam, W. G., and J. Y. L. Chiang. 1992. Polymorphisms of human cholesterol 7α-hydroxylase. *Biochem. Biophys. Res. Commun.* **185:** 588–595.
19. Setchell, K. D. R., M. Schwarz, N. C. O'Connell, E. G. Lund, D. L. Davis, R. Lathe, H. R. Thompson, R. Weslie Tyson, R. J. Sokol, and D. W. Russell. 1998. Identification of a new inborn error in bile acid synthesis: mutation of the oxysterol 7α-hydroxylase gene causes severe neonatal liver disease. *J. Clin. Invest.* **102:** 1690–1703.
20. Mizuno, M., and M. Kanehisa. 1994. Distribution profiles of GC content around the translation initiation site in different species. *FEBS Lett.* **352:** 7–10.
21. Schwarz, M., E. G. Lund, R. Lathe, I. Bjorkhem, and D. W. Russell. 1997. Identification and characterization of a mouse oxysterol 7α-hydroxylase cDNA. *J. Biol. Chem.* **272:** 23995–24001.
22. Quandt, K., K. Frech, H. Karas, E. Wingender, and T. Werner. 1995. MatInd and MatInspector: new fast and versatile tools for detection of consensus matches in nucleotide sequence data. *Nucleic Acids Res.* **23:** 4878–4884.
23. Wang, X., R. Sato, M. S. Brown, X. Hua, and J. L. Goldstein. 1994. SREBP-1, a membrane-bound transcription factor released by sterol-regulated proteolysis. *Cell.* **77:** 53–62.
24. Flanagan, W. M., B. Corthesy, R. J. Bram, and G. R. Crabtree. 1991. Nuclear association of a T-cell transcription factor blocked by FK-506 and cyclosporin A. *Nature.* **352:** 803–807.
25. Lenardo, M. J., and D. Baltimore. 1989. NF-KB: a pleiotropic mediator of inducible and tissue-specific gene control. *Cell.* **58:** 227–229.
26. Whyatt, D. J., E. deBoer, and F. Grosveld. 1993. The two zinc finger-like domains of GATA-1 have different DNA binding specificities. *EMBO J.* **12:** 4993–5005.
27. Xanthopoulos, K. G., V. R. Prezioso, W. S. Chen, F. M. Sladek, R. Cortese, and J. E. Darnell. 1991. The different tissue transcription patterns of genes for HNF1, C/EBP, HNF3, and HNF4 protein factors that govern liver-specific transcription. *Proc. Natl. Acad. Sci. USA.* **88:** 3807–3811.
28. Rosenfeld, P. J., and T. J. Kelly. 1986. Purification of nuclear factor I by DNA recognition site affinity chromatography. *J. Biol. Chem.* **261:** 1398–1408.
29. Li, Y. C., and J. Y. L. Chiang. 1991. The expression of a catalytically active cholesterol 7a-hydroxylase cytochrome P450 in *E. coli*. *J. Biol. Chem.* **266:** 19186–19191.
30. Nelson, D. R., T. Kamataki, D. J. Waxman, F. P. Guengerich, R. W. Estabrook, R. Feyereisen, F. J. Gonzalez, M. J. Coon, I. C. Gunsalus, O. Gotoh, K. Okuda, and D. W. Nebert. 1993. The P450 superfamily: update on new sequences, gene mapping, accession number, early trivial names of enzymes, and nomenclature. *DNA Cell Biol.* **12:** 1–51.
31. Norlin, M., and K. Wikvall. 1998. Biochemical characterization of the 7α-hydroxylase activities towards 27-hydroxycholesterol and dehydroepiandrosterone in pig liver. *Biochim. Biophys. Acta.* **1390:** 269–281.
32. Brown, A. J., and W. Jessup. 1999. Oxysterols and atherosclerosis. *Atherosclerosis.* **142:** 1–28.
33. Goldstein, J. L., and M. S. Brown. 1990. Regulation of the mevalonate pathway. *Nature.* **343:** 425–430.
34. Janowski, B. A., P. J. Willy, T. R. Devi, J. R. Falck, D. and J. Mangelsdorf. 1996. An oxysterol signaling pathway mediated by the nuclear receptor LXRα. *Nature.* **383:** 728–731.
35. Baulieu, E. E., and P. Robel. 1998. Dehydroepiandrosterone (DHEA) and dehydroepiandrosterone sulfate (DHEAS) as neuroactive neurosteroids. *Proc. Natl. Acad. Sci. USA.* **95:** 4089–4091.
36. Compagnone, N. A., and S. H. Mellon. 1998. Dehydroepiandrosterone: a potential signaling molecule for neocortical organization during development. *Proc. Natl. Acad. Sci. USA.* **95:** 4678–4683.
37. Robel, P., and E. E. Baulieu. 1995. Dehydroepiandrosterone (DHEA) is a neuroactive neurosteroid. *Ann. NY Acad. Sci.* **774:** 82–110.
38. Wang, H., J. Chen, K. Hollister, L. C. Sowers, and B. M. Forman. 1999. Endogenous bile acids are ligands for the nuclear receptor FXR/BAR. Mol. *Cell.* **3:** 543–553.
39. Makishima, M., A. Y. Okamoto, J. J. Repa, H. Tu, R. M. Learned, A. Luk, M. V. Hull, K. D. Lustig, D. J. Mangelsdorf, and B. Shan. 1999. Identification of a nuclear receptor for bile acids. *Science.* **284:** 1362–1365.
40. Parks, D. J., S. G. Blanchard, R. K. Bledsoe, G. Chandra, T. G. Consler, S. A. Kliewer, J. B. Stimmel, T. M. Willson, A. M. Zavacki, D. D. Moore, and J. M. Lehmann. 1999. Bile acids: Natural ligands for an orphan nuclear receptor. *Science.* **284:** 1365–1368.